ELSEVIER

Contents lists available at ScienceDirect

Digital Applications in Archaeology and Cultural Heritage

journal homepage: www.elsevier.com/locate/daach



3D scanning of antique glass by combining photography and computed tomography



Peter Fried a,*, Jonathan Woodward b, David Brown c, Drew Harvell d, James Hanken b

- a Dept. of Applied Physics, NYU Tandon School of Engineering, Six Metrotech Center, Brooklyn, NY, 11201, USA
- ^b Museum of Comparative Zoology, Harvard University, 26 Oxford St, Cambridge, MA, 02138, USA
- ^c Herbert F. Johnson Museum of Art, Cornell University, 114 Central Ave, Ithaca, NY, 14853, USA
- d Department of Ecology and Evolutionary Biology, Cornell University, E145 Corson Hall, Ithaca, NY, 14853, USA

ARTICLE INFO

Keywords:
Photogrammetry
X-ray computed tomography
3D-models
Blaschka glass models

ABSTRACT

We demonstrate archival 3D digitization of glossy, translucent and highly detailed glass sculptures, namely the glass models of marine invertebrates made by Rudolf and Leopold Blaschka in the late 19th century. Achieving satisfactory results required optimizing well-known techniques of light and polarization control and photogrammetric processing. Significantly, we in addition merged photogrammetry and X-ray computed tomographygenerated meshes to digitize detailed sculptures made of multiple materials including glass. These techniques should enable the 3D-digitization of objects heretofore considered challenging for 3D scanning.

1. Introduction

An increasing number of museums are using 3D imaging both for archival recording and to allow the global public to experience objects in collections that they would otherwise never be able to get close to. Photogrammetry, optical scanning and X-ray computed tomography (CT) scanning are all being used (Hancock, 2015; Metallo and Rossi, 2011). These efforts benefit from steadily improving technology and abundant software options, and they build on extensive earlier work done primarily in archaeological, zoological and biomedical applications (Gutiérrez et al., 2018; Mallison et al., 2014; Ziegler et al., 2018). Notable efforts are those at the Smithsonian Institution (Metallo and Rossi, 2011; Alba, 2018) and The British Museum (https://sketchfab.com/britishmuseum).

However, rendering 3D images that are faithful to the original object remains difficult for many specimens. Fine detail or lack of detail, thin structures, hidden or glossy surfaces, and transparent or semi-transparent volumes are a few of the challenges. Intricate antique glasswork, while especially challenging for 3D imaging, also benefits tremendously from it because the specimens are typically very fragile; for conservation reasons, they should be handled as little as possible, if at all. For the last three years we have been making 3D images of the intricate and beautiful glass models of marine invertebrates created between 1863 and 1890 by the father and son team of Leopold and Rudolf Blaschka (Brill et al., 2016; Harvell, 2016).

The Blaschkas made thousands of these models, principally as teaching aids. They were shipped from the Blaschkas' workshop in Dresden, Germany, to universities, schools and museums around the world. The Blaschkas made their models based on their own extensive observations of living animals in aquaria and during several ocean voyages, and also based on drawings by contemporary taxonomists. The glass models of soft marine invertebrates were especially valuable because the shape and color of live specimens did not preserve well after death in fixatives used at that time. These models serve as a record of ocean life 100 or more years ago, and therefore are valuable to studies of evolution and the impacts of climate change.

Today, the principal collections of Blaschka marine invertebrate models are at Cornell University (Harvell, 2016), the Harvard Museum of Comparative Zoology (MCZ; Brill et al., 2016), the Corning Glass Museum, and University College, Dublin (Doyle et al., 2017). Many smaller collections exist at institutions around the world (Ruggiero and Larson, 2017). For the present study, we have imaged models at Cornell (Prof. Drew Harvell, curator) and MCZ (Prof. James Hanken, director)

2. Materials and methods

Our imaging work began with glass models that are relatively simple in form and completely painted (Figs. 1–3), so as to develop the basic photogrammetry workflow required, e.g., the minimum numbers of

E-mail addresses: pf736@nyu.edu (P. Fried), jwoodward@oeb.harvard.edu (J. Woodward), dbrownpix@gmail.com (D. Brown), cdh5@cornell.edu (D. Harvell), hanken@oeb.harvard.edu (J. Hanken).

^{*} Corresponding author.

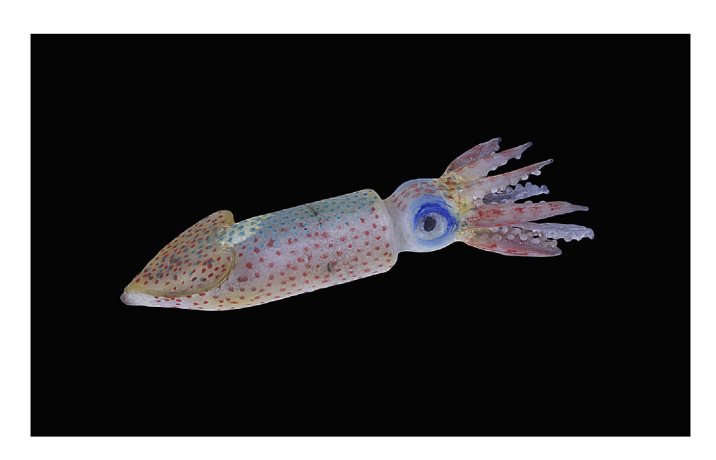


Fig. 1. European squid, Loligo berthelotii. Model B-560 of the Cornell University Collection of Blaschka Marine Invertebrates (length ~ 6.4 cm) (3D view: htt ps://skfb.ly/6Mwtq).



Fig. 2. Fontaine's octopus, *Robsonella fontanianus*. Model SC-380 of the Harvard Museum of Comparative Zoology collection of Blaschka marine invertebrates (spanning 13 cm from arm to arm) (3D view: https://skfb.ly/6H7ZN).



Fig. 3. Stout bobtail squid, *Rossia macrosoma*. Model B-588 of the Cornell University Collection of Blaschka Marine Invertebrates (length ~ 15 cm) (3D view: https://skfb.ly/6NrwZ).

photographs and angles needed to yield high-resolution images. We then optimized control of the lighting, especially polarization, using somewhat more complicated models that include sections of bare glass and/or glossy paint (Figs. 4–6). Finally, there are some models with substantial transparent areas and/or intricate detail for which photogrammetry



Fig. 4. Sea anemone, *Phymactis pustulata*. Model SC-51 of the Harvard Museum of Comparative Zoology collection of Blaschka marine invertebrates (width \sim 10 cm) (3D view: https://skfb.ly/6IyHS).



Fig. 5. Greater argonaut, Argonauta argo. Model SC-363 of the Harvard Museum of Comparative Zoology collection of Blaschka marine invertebrates (length \sim 7 cm) (3D view: https://skfb.ly/6Nrxo).

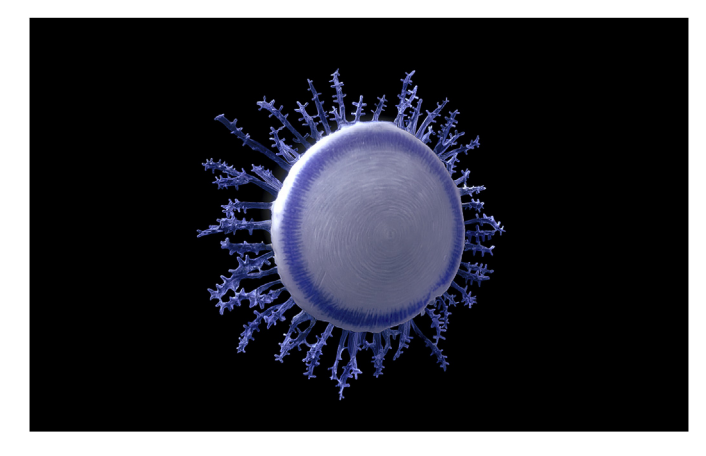


Fig. 6. Blue button jellyfish, *Porpita porpita*. Model SC-138 of the Harvard Museum of Comparative Zoology collection of Blaschka marine invertebrates (diameter ~ 7 cm) (3D view: https://skfb.ly/6Nrx7). (For interpretation of the references to color in this figure legend, the reader is referred to the Web version of this article.)

alone is inadequate (Fig. 7). For these models, we generated meshes with both photogrammetry and X-ray CT scanning, which were then combined to create the final reconstruction.



Fig. 7. Football sea squirt, *Diazona violacea*. Model SC-418 of the Harvard Museum of Comparative Zoology collection of Blaschka marine invertebrates (width ~ 9 cm). The high definition of the digital model results from a mesh made from a CT scan. This was aligned and merged in Agisoft Metashape with a mesh made from 699 photographs. The combined mesh was then textured from the photos (3D view: https://skfb.ly/6LxKy).

2.1. Camera angles and alignment

The photogrammetry involved between 250 and 700 photographs of each glass model, which were taken against a black background on a turntable using 2–4 different camera angles. When possible, the model was arranged on the turntable in several different orientations to achieve 2–3 more or less orthogonal axes of rotation. A large number of photographs is needed both to insure good inter-photo registration, or "alignment," and to insure adequate coverage of the entire complex geometry of the models. To further insure proper alignment, distinct colored targets were mounted on the turntable, away from the glass model, near the edge of the field of view.

2.2. Lighting and exposure

Traditionally, specular reflections are minimized by applying a powder or spray coating to the subject. Such treatment, however, is not possible for the Blaschka models, especially in view of the fragile organic paints used to manufacture many of them. Controlling the polarization of incident light by applying filters to the lens and/or the lights themselves can also be used to minimize (or maximize) specular reflections.

The final position of the camera and lights was a compromise among the polarization control and additional issues:

- The need for high resolution
- The need to maximize relative depth of field
- The need to minimize exposure time
- · Available resources, including lenses and controllable polarizers

For the 3D models illustrated in this paper, we used a 55 W, 14″-diameter ring light and a Nikon 7100 DSLR camera with an 80- or 90-mm macro lens. Lights and lens were located between one and three feet from the turntable. Apertures of f11–f20 were generally used. The camera, mounted on a firm tripod, was usually operated by remote control and typically set at a high ISO value (1600–2500). Excessive sensor noise can sometimes degrade inter-image alignment, but this did not appear to be the case at these ISO values. For some models, we were able to operate the turntable continuously at 1 rpm while making 1/50- or 1/25-sec exposures every 0.5–1.0 s. However, crossed polarizers on the lens and ring light were used when necessary to control specular reflections, and this procedure required longer exposures (e.g., ¼–1/10 sec) and, hence, manual stepping of the turntable.

2.3. Photogrammetry processing

Among the many different software packages currently available, we used Agisoft Photoscan (recently updated and renamed Metashape). This software is affordable, completes the processing locally and has a good user interface that allows the user to control the separate processing steps in a manner suitable for this work. The software is used on a Dell Precision Mobile Workstation M4800 with 32 GB of RAM, an Intel Core i7-4910MQ Processor running at 2.9 GHz, and an NVIDIA Quadro K2100M Graphics card with a clock rate of 666 MHz.

Key factors that affect processing time are the number of photos, the number of pixels in the unmasked portion of each photo, and the required accuracy level. Table 1 shows selected metrics on processing time, point counts and accuracy levels from the Agisoft software for the 3D models illustrated in this paper. The most challenging step in the photogrammetry, but not necessarily the most time-consuming, was always the inter-photo alignment. For several models, we included alignment targets off the model at the edge of the turntable. These were useful as long as the model's orientation on the turntable remained unchanged. To align photos of a given model in multiple orientations, in one case we created separate partial digital models—"chunks," in the Agisoft nomenclature—for each orientation and then merged the chunks. In other cases, we used the off-model alignment targets in one orientation and masked them in others to achieve a successful alignment. In any event, the software occasionally failed to align or created erroneous alignments due to accumulated small errors. Solving these cases involved various combinations of (a) adding more photos, (b) removing selected photos, (c) reordering photos, and (d) sequential re-alignments of subsets of photos. The highest-accuracy mode, which also is the most time-consuming, was usually required to successfully align the large number of photographs.

Generating the dense point cloud, meshing the model and texturing usually proceeded routinely. These steps are also summarized in Table 1.

2.4. X-ray CT scanning and processing

As stated earlier, there were some glass models for which even the techniques described above would not yield satisfactory results. Typically, these combine complex design with hidden or partially hidden surfaces, transparent or semi-transparent sections, and/or significant specular reflecting surfaces (e.g., Fig. 7). For these glass models, we generated an X-ray computed-tomography (CT) scan that would be combined with a photogrammetry scan of the same specimen. 3D reconstruction from CT data has been extensively developed for metrology and biomedical applications (Khan et al., 2018)

For CT scanning, we mounted the glass model on an archival foam block, stabilizing it with Parafilm strips wrapped around archival cotton pads. We scanned the model using a Bruker Skyscan 1173 Micro-CT Scanner, with a source voltage of 105 kV and a source current of 60 $\mu A.$ We interposed a 1.0 mm aluminum filter to reduce scatter artifacts in the final model.

For reconstruction of the CT scan (creating slice images) and 3D model building, we used NRecon and CTAn, respectively (each is part of the Bruker "3D.SUITE" software package). The slice images went through an initial thresholding step to separate the model from the background, a de-speckling step aimed at further reducing noise, and a model-creation step that resulted in an STL surface model file. Finally, in Meshlab, we manually removed islands of artifact noise before downsampling (for ease of use) using Quadric Edge Collapse Decimation.

The greatest challenges encountered during the micro-CT scan and reconstruction were attributable to the very thin and relatively radio-transparent glass of the Blaschka models. Several scanning attempts were required to achieve a set of slice images in which the model could be cleanly thresholded from the background. After even the best of these attempts, several levels of noise reduction (as mentioned above) were necessary.

Table 1
Selected metrics for the photogrammetry processing of the models depicted in Figs. 2–7. The Point Cloud, Dense Cloud and Mesh Model metrics are all taken from the Agisoft software, either Photoscan or Metashape. Metrics are not shown for Fig. 1, the B-560 cephalopod, because it was the first model undertaken and was the combined result of multiple processing runs.

	Model	SC-380 Octopus	B-588 Rossia pacifica	SC-51 Anemone	SC-363 Argonaut	SC-138 Porpita	SC-418 Tunicate
Figure #	2	3	4	5	6	7	
	Approximate Size (cm)	13 (armspan)	15	10	7	7	5
	Photos	300	454	220	405	352	699 (+CT data)
	Agisoft Software Version	1.2.6	1.3.3	1.4.0	1.4.4	1.3.3	1.5.0
Point Cloud &	Aligned photos	287	340	220	405	328	699
Alignment	Points	88,739 of	65,803 of 82,555	52,150 of	130,222 of	106,754 of	181,565 of
		133,425		63,283	143,899	125,335	203,011
	RMS reprojection error	0.25 (1.50 pix)	0.145 (0.82 pix)	0.13 (1.13 pix)	0.24 (0.87 pix)	0.17 (1.02 pix)	0.21 (1.83 pix)
	Mean key point size	5.6 pix	4.9 pix	7.6 pix	3.6 pix	5.5 pix	8.3 pix
	Average tie point multiplicity	3.5	3.99	3.0	3.8	3.0	3.6
	Matching time (min)	53.2	74	37.3	40.3	37.7	92
	Alignment time (min)	0.05	1.4	0.5	9.5	2	14.6
Dense Cloud	Points (Millions)	2.45	1.06	5.96	1.87	0.90	6.93
	Quality	High	Medium	High	High	Medium	High (350 photos)
	Depth maps time (min)	189	41	80	219	23.5	152
	Dense cloud time (min)	375	75	222	387	98	888
Mesh Model	Faces (Millions)	0.49	0.071	0.21	0.37	0.060	0.20
	Vertices	244,647	35,334	104,972	186,970	30,035	99,984
	Quality	High	Medium	High	High	Medium	High
	Face count (Millions)	0.49	0.071	1.19	0.37	0.060	1.39
	Processing time (min)	1.7	0.5	28.5	10.3	0.7	5.9
	UV map & Texture time (min)	3	6.5	3.5	10	7	13.5
	Display face count (Millions)	0.49	0.070	0.21	0.17	0.32	1.00

2.5. Merging photo-generated and CT-generated information

For some complex models, the mesh can be defined entirely by the X-ray CT data. Any surface coloring, however, such as that in the texture file, must be provided by photographic data. For other models, certain parts of the structure are made of paint and other filler materials, which are radiotransparent (e.g., Fig. 7). These parts must be defined with photogrammetry meshes that are then merged with the X-ray-generated sections (Fig. 8). For the model shown in Fig. 7, the reconstruction obtained by using only the X-ray CT data is shown in Fig. 8a. The upper unpainted sections are well defined, but the organic paints used in the lower section are not seen because they were not detected by the X-ray CT scan. Conversely, Fig. 8b depicts the reconstruction made just from the photographic data. The lower painted section is well modeled here, but the upper glassy sections confuse the photogrammetry and are poorly processed.

The workflow for models such as that shown in Fig. 7 is described here. Although the specific steps apply to Agisoft Metashape and Blender, they should be similar for other software choices.

- Two meshes were created separately, one from photographs and a second from CT data.
- 2. In the case of the model of the football sea squirt (Fig. 7), the X-ray-generated mesh had 6 million faces. Using Blender, this mesh was first decimated to one million faces and then scaled, rotated and translated so that it roughly aligned with, and had the same reference frame as, the photo-mesh.
- 3. The X-ray mesh, newly scaled and moved, was exported from Blender as an.stl or.obj file. Using the Agisoft software, it was fine-aligned to the photo-generated mesh.
- 4. If the entire mesh was to be defined by the CT data, then (a) the photo-generated mesh was discarded and (b) a texture file was built from the photos and mapped to the surface of the CT mesh. Erolin et al. (2017) demonstrate the use of CT-generated meshes that are then "painted" with photographic surface information by using software such as Z-brush. In the present work, with a common frame of

- reference for the CT-generated mesh and the photographs, we were able to use the photos to accurately create the texture file.
- 5. If a combination of the photo-generated and the x-ray meshes was required (e.g., Fig. 7), the two meshes were brought back to Blender, where the unwanted parts of each one were discarded and the remaining parts joined into one mesh. Finally, this resulting mesh was exported to Metashape, where the photographs were used to build the texture file.

2.6. Post-processing of the models

Some models required no additional work after the mesh and texture files were completed. Others, however, required post-processing, which was done with Blender.

- a) The "Sculpt" mode in Blender provides tools for smoothing portions of the mesh, removing distortions and improving the definition of narrow crevices.
- b) Blender can also be used to divide the mesh into sections of different materials (defined by the.mtl files). This allows for different levels of transparency and translucence, albedo, roughness and surface gloss.

3. Results and discussion

Once post-processing was complete the 3D files were uploaded to the SketchFab viewer where, after adding a background and appropriate lighting, we adjusted surface qualities of the model. Some of the resulting 3D models are shown in Figs. 1–7. The complete set (15 models to date) can be seen at https://sketchfab.com/ARC-3D.

Our objective is to demonstrate archival capture of challenging 3D subjects, specifically glossy, translucent and highly detailed and delicate glass models. Much of our workflow optimizes well-known techniques of light and polarization control and photogrammetric processing. Significantly, we have also merged photogrammetry and CT data to create meshes of intricate structures made of multiple materials including glass.

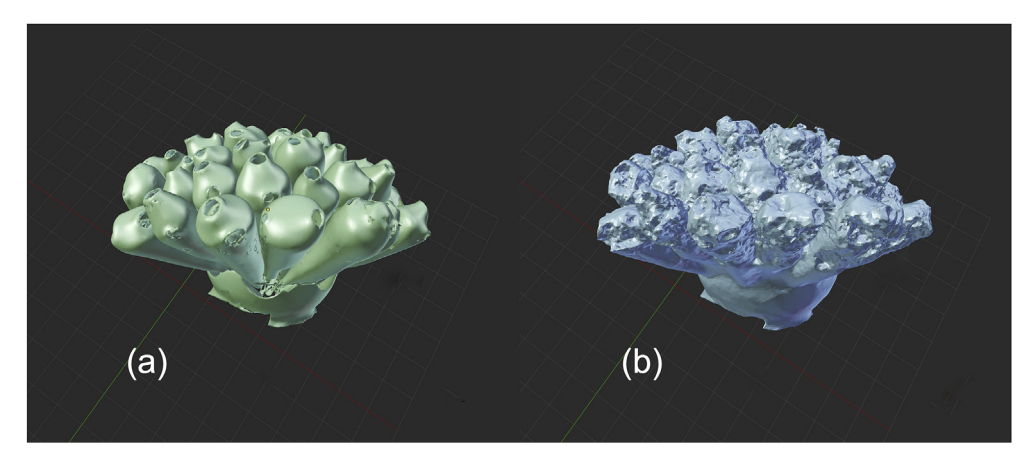


Fig. 8. Partial reconstructions of the football sea squirt, *Diazona violacea* in a similar orientation to Fig. 7. (a) The reconstruction created by using only X-ray data, and (b) the reconstruction created by using only photographic data.

Recently, software and cameras have become available with automated focus stacking (Kontogianni et al., 2017). This feature holds promise for some combination of higher resolution, larger effective depth of field and shorter individual exposures, but only if the processing load for 250–700 separate photos is manageable.

Future work should (a) identify ways to improve efficiency and resolution through focus stacking; (b) develop further use of CT scanning, especially for imaging highly transparent glassworks (e.g., Blaschka jellyfish); and (c) explore the utility of voxel-based processing for digitizing such objects. The use of these additional techniques, as well as those demonstrated herein, should expand the universe of objects suitable for 3D digitization.

Declaration of competing interest

None.

CRediT authorship contribution statement

Peter Fried: Conceptualization, Investigation, Methodology, Visualization, Writing - original draft, Writing - review & editing. Jonathan Woodward: Investigation, Methodology, Writing - review & editing. David Brown: Investigation, Methodology, Visualization. Drew Harvell: Resources, Supervision, Project administration. James Hanken: Resources, Supervision, Project administration, Writing - review & editing.

Acknowledgements

This work was made possible by the hospitality and access to collections provided by the staff of the Harvard Museum of Comparative Zoology and the Cornell University Department of Ecology and Evolutionary Biology. For valuable advice on photography, photogrammetry and CT scanning, we thank Taylor Shields, New York University LaGuardia Studio; Heinrich Mallison, Museum für Naturkunde, Berlin,

Germany; Teresa Porri, Manager of the Cornell Biotechnology Resource Center Imaging Facility; Victoria Bill, Manager of the New York University Tandon MakerLab; and Thomas Flynn, Sketchfab.

This research was supported by the Harvard Museum of Comparative Zoology and NSF award no. DBI-1702263 to J.H., and by the Cornell University Blaschka Collection.

References

Alba, M., 2018. 3D Scanning the Past at the Smithsonian. Engineering.Com, October 11, 2018. https://www.engineering.com/Hardware/ArticleID/17765/3D-Scanning-the -Past-at-the-Smithsonian.aspx.

Brill, E.R., Huber, F., Brown, D.O., 2016. Sea Creatures in Glass: the Blaschka Marine Animals at Harvard. Scala Arts Publishers, New York.

Doyle, H., Callaghan, E., Reynaud, E.G., 2017. Blaschka invertebrate models in Irish institutions. J. Hist. Collect. 29, 439–450. https://doi.org/10.1093/jhc/fhw030.

Erolin, C., Jarron, M., Csetenyi, L.J., 2017. Zoology 3D: creating a digital collection of specimens from the D'Arcy Thompson Zoology Museum. Digit. Appl. Archaeol. Cult. Herit. 7, 51–55. https://doi.org/10.1016/j.daach.2017.11.002.

Gutiérrez, Y., Ott, D., Töpperwien, M., Salditt, T., Scherber, C., 2018. X-ray computed tomography and its potential in ecological research: a review of studies and optimization of specimen preparation. Ecol. Evol. 8, 7717–7732.

Hancock, M., 2015. Museums and 3D printing: more than a workshop novelty,
 Connecting to collections and the classroom. Bull. Assoc. Inf. Sci. Technol. 42, 32–35.
 Harvell, D., 2016. A Sea of Glass. University of California Press, Oakland.

Khan, U., Yasin, A., Abid, M., Shafi, I., Khan, S.A., 2018. A methodological review of 3D reconstruction techniques in tomographic imaging. J. Med. Syst. 42, 190. https://doi.org/10.1007/s10916-018-1042-2.

Kontogianni, G., Chliverou, R., Koutsoudis, A., Pavlidis, G., Georgopoulos, A., 2017. Enhancing close-up image-based 3D digitisation with focus stacking. Int. Arch. Photogram. Rem. Sens. Spatial Inf. Sci. 421–425. Volume XLII-2/W5, 26th International CIPA Symposium, 28 August–01 September 2017. Ottawa, Canada.

Mallison, H., Vogel, J., Belvedere, M. (Eds.), 2014. Digital Specimen 2014 - Abstracts of Presentations. Museum für Naturkunde Berlin. http://www.naturkundemuseum.be rlin/sites/default/files/digitalspecimen2014_abstracts_of_presentations_01.pdf.

Metallo, A., Rossi, V., 2011. The future of three-dimensional imaging and museum applications. Curator 54, 63–69. https://onlinelibrary.wiley.com/doi/full/10.1111 /i.2151-6952.2010.00067.x.

Ruggiero, A., Larson, K.A., 2017. The Blaschka legacy in worldwide collections: a new resource. J. Glass Stud. 59, 419–428. www.jstor.org/stable/90013844.

Ziegler, A., Bock, C., Ketten, D.R., Mair, R.W., Mueller, S., Nagelmann, N., Pracht, E.D., Schröder, L., 2018. Digital three-dimensional imaging techniques provide new analytical pathways for malacological research. Am. Malacol. Bull. 36, 248–273.